

# Lifetime measurements on the $c'_4{}^1\Sigma_u^+$ , $v = 0, 1$ and $2$ states of molecular nitrogen

W. Ubachs<sup>a,\*</sup>, R. Lang<sup>a,b</sup>, I. Velchev<sup>a</sup>, W.-Ü.L. Tchang-Brillet<sup>c,d</sup>,  
A. Johansson<sup>e</sup>, Z.S. Li<sup>e</sup>, V. Lokhnygin<sup>e</sup>, C.-G. Wahlström<sup>e</sup>

<sup>a</sup> Department of Physics and Astronomy, Laser Centre, Vrije Universiteit, De Boelelaan 1081, 1081 HV Amsterdam, Netherlands

<sup>b</sup> FOM-institute for Atomic and Molecular Physics, Kruislaan 407, 1098 SJ Amsterdam, Netherlands

<sup>c</sup> Département DAMAP, UMR8588 du CNRS, Observatoire de Paris-Meudon, F-92195 Meudon Cedex, France

<sup>d</sup> Université Pierre et Marie Curie (Paris 6), Paris, France

<sup>e</sup> Department of Physics, Lund Institute of Technology, P.O. Box 118, S-221 00 Lund, Sweden

Received 19 February 2001

## Abstract

Excited state lifetimes of  $c'_4{}^1\Sigma_u^+$ ,  $v = 0$ – $2$  states of molecular nitrogen have been determined in a laboratory investigation using a picosecond XUV laser in a pump–probe configuration. For  $c'_4{}^1\Sigma_u^+$ ,  $v = 0$  the lifetime is  $\tau = 740 \pm 50$  ps, for the lowest rotational states. For higher rotational states a gradual shift towards  $\tau = 495$  ps is found in agreement with previous findings that these states are subject to predissociation. For  $c'_4{}^1\Sigma_u^+$ ,  $v = 1$  no  $J$ -dependence is found and values for two isotopomers are reported:  $\tau = 330$  ps for  $^{14}\text{N}_2$  and  $\tau = 240$  ps for  $^{14}\text{N}^{15}\text{N}$ . For  $c'_4{}^1\Sigma_u^+$ ,  $v = 2$  a lifetime for the lowest rotational states ( $J = 0$ – $3$ ) was derived:  $\tau = 675 \pm 50$  ps; for  $J = 11$  a lifetime of  $\tau \leq 120$  ps is deduced. All values for the lifetimes including the  $J$ -dependences are explained in a model based on Rydberg-valence interaction. © 2001 Elsevier Science B.V. All rights reserved.

## 1. Introduction

The lowest Rydberg states of  ${}^1\Sigma_u^+$  symmetry of molecular nitrogen are the prime extreme ultraviolet (XUV) absorbers in the Earth's atmosphere [1]. From laboratory experiments it has been established that specifically excitation to the  $c'_4{}^1\Sigma_u^+$ ,  $v = 0$  state of  $\text{N}_2$ , also indicated as  $c'_4(0)$ , carries the largest absorption oscillator strength of all dipole allowed transitions. Moreover upon electron-induced collisional excitation, occurring in

the upper layers of the atmosphere, the  $c'_4(0,0)$  band has the largest fluorescence cross section [2]. This band was reported, in the Voyager-I space mission, as the strongest XUV-emission feature in the atmosphere of Titan, predominantly consisting of molecular nitrogen [3]. However, Stevens has recently argued that this reported result of  $c'_4(0,0)$  as the strongest XUV-emission feature is based on a misidentification and it is proposed that a variety of features, including those from excited nitrogen atoms, are responsible for the intense emission peak near 95.8 nm [4]. The  $c'_4(0,0)$  band as well as the other prominent absorption and emission bands pertaining to molecular nitrogen are all in the spectroscopic window covered by the high

\* Corresponding author. Fax: +31-20-4447999.  
E-mail address: wimu@nat.vu.nl (W. Ubachs).

resolution spectrometer aboard the new NASA Far Ultraviolet Spectroscopic Explorer (FUSE) satellite, in orbit since mid-1999. The presently reported laboratory studies on the decay properties of Rydberg states of  $N_2$  bear relevance for this FUSE project as well as for the Cassini Mission on its way to Titan. The resolution of the spectrometer aboard Cassini is high enough to unravel the atomic and molecular emission features near 96 nm.

The emission and dissociation properties of the excited states of  $^1\Sigma_u^+$  and  $^1\Pi_u$  symmetry in  $N_2$  have been extensively discussed in the literature, often in connection with phenomena occurring in the Earth's atmosphere, such as the dayglow, the nightglow and the aurora processes. Key issue has been to determine the relative rates of the competing processes of emission and predissociation, after photo-absorption or electron collisional excitation; this is intimately connected with the rate of production of N-atoms and the chemistry in the upper layers in the atmosphere. In early experiments by Zipf and McLaughlin [5] it was found that the predissociation probability of the  $c'_4(^1\Sigma_u^+)$  Rydberg state, a crucial parameter for the modeling of atmospheres, was 15%, for the vibrational levels  $v' = 0-4$  and over 95% for levels  $v = 5-7$ . In later studies by Ajello et al. [2] the predissociation yield was found to be less than 10% for  $c'_4$  vibrational levels. Additional rotationally resolved measurements [6] gave a predissociation yield of 16.2%, specifically for the  $c'_4(0)$  state at temperatures of 400 K. Moreover an increasing predissociation was obtained for higher rotational quantum numbers. Such low predissociation yields could however not be reconciled with observed XUV emissions of the Earth's atmosphere; this led to a problem referred to as the missing radiation problem by Stevens et al. [7]. The authors were able to resolve this issue by invoking a delicate interference between emission in the  $c'_4(0,1)$  band and reabsorption in the  $b^1\Pi_u-X(2,0)$  band. Since the  $b^1\Pi_u, v = 2$  excited state was known to be subject to rapid predissociation [8] multiple scattering in an optically dense atmosphere could help to explain the loss of XUV photons; equally important in the model of Stevens et al. was the treatment of radiative trapping in the Earth's

atmosphere. Slanger reanalyzed near ultraviolet spectra of the Earth's aurora and was able to identify emission bands in the Gaydon–Herman system originating from the  $c'_4(0)$  upper state, in particular the  $c'_4(^1\Sigma_u^+)-a^1\Pi_g(0,4)$  and  $(0,5)$  bands [9]. Quantitative emission measurements have yielded a branching ratio of only 1.1% for decay into the  $a^1\Pi_g$  state [2].

The spectroscopy of the dipole accessible excited states of  $N_2$  is complicated and was not understood for a long time. The  $c'_4(^1\Sigma_u^+)$  state is the lowest member of the  $np\sigma_u$  Rydberg series, which was investigated over the years [10–12]. The highest resolution study on some rotational lines in the  $c'_4(0,0)$  band was recently performed, using a narrow-band XUV laser, with a resolving power of  $6.2 \times 10^7$  [13]. It was through the pivotal work of Stahel et al. [14] that the spectrum of the excited singlet states of  $N_2$  became understood and set on a firm quantitative basis. Strong homogeneous perturbations between the Rydberg manifolds of  $^1\Sigma_u^+$  and  $^1\Pi_u$  symmetry and the  $b^1\Sigma_u^+$  and  $b^1\Pi_u$  valence states could explain the large level shifts and the absorption strengths deviating from the normal Franck–Condon behavior. Later this picture was filled in with details. The local perturbation between the  $c'_4(^1\Sigma_u^+, v = 0)$  and  $b^1\Sigma_u^+, v = 1$  states was analyzed by Yoshino and Tanaka [15] and later, in higher resolution laser excitation, by Levelt and Ubachs [16]. The effect of heterogeneous couplings between states of different symmetry has to be included as well as was shown by Yoshino and Freeman [17] for a limited wavelength interval. The interaction of states with  $np\sigma_u$  and  $np\pi_u$  Rydberg orbitals, resulting in  $c'_{n+1}(^1\Sigma_u^+)$  and  $c_n(^1\Pi_u)$  states, was analyzed in terms of a  $p$ -complex by Carroll and Yoshino [11]. Levelt and Ubachs [16] had also included the interaction of the  $c_3(^1\Pi_u, v = 0)$  state on the  $c'_4(^1\Sigma_u^+, v = 0)$  state. An extended analysis, including homogeneous and heterogeneous effects, between all Rydberg and valence states of  $^1\Sigma_u^+$  and  $^1\Pi_u$  symmetry was performed by Edwards et al. [18]; such a model should in principle explain rotationally dependent effects in lifetimes, oscillator strengths and predissociation yields.

Lifetime measurements on  $c'_4(0)$  were performed by various groups using different techniques [13, 19]. Oertel et al. [20] have reported lifetimes for the

$c'_4(0)$  and  $c'_4(2)$  levels, while Kam et al. [21] measured  $c'_4(3)$  lifetimes from line broadening. Helm et al. [22] observed strong rotational effects on the lifetimes of  $c'_4(4)$ , also from line broadening. Ajello et al. [23] included these data to derive the predissociation yield for both the  $c'_4(3)$  and  $c'_4(4)$  states, again with strong rotational state dependences. In the present paper we report on the application of an alternative technique for measurement of excited state lifetimes. A two-laser pump–probe experiment is performed to derive lifetimes of the lowest three vibrational levels  $v = 0–2$  of the  $c'_4{}^1\Sigma_u^+$  Rydberg state.

## 2. Experimental method

Direct time-domain measurements of excited state lifetimes are performed by 1XUV + 1UV two-photon ionization. A tunable and pulsed coherent XUV laser system is used to resonantly excite the state under investigation and a time-delayed pulsed UV laser is used, in a pump–probe configuration, to photoionize the excited molecules. A description of the picosecond XUV source of the Lund Laser Centre, including its temporal and bandwidth characteristics, was described previously by Larsson et al. [24], while its application to similar lifetime measurements on some excited states of CO was reported by Cacciani et al. [25]. The XUV pulses are generated by a chain involving a distributed-feedback dye laser (DFDL), a titanium–sapphire amplifier and harmonic generation, running at 10 Hz repetition rate. The amplified tunable IR pulses have a duration of  $\approx 90$  ps, as measured on a streak camera and a pulse energy of up to 50 mJ. They are frequency doubled in a KD\*P crystal. The combined output of the leftover IR and UV pulses are focused into a pulsed krypton jet for harmonic generation. The eighth harmonic of the IR input wavelength is produced in a nonlinear mixing process, e.g. through  $\nu_{\text{XUV}} = 3\nu_{\text{UV}} + 2\nu_{\text{IR}}$ , and is selected by a spherical grating and refocused into the interaction region. By tuning the DFDL, accomplished by varying the temperature of the dye solution inside the laser, the XUV radiation can be tuned into resonance with an absorption of  $\text{N}_2$ . A pulsed

laser spectrum analyzer is used on-line to measure the absolute wavelength and the bandwidth of the IR laser, which was determined at  $\Delta\lambda_{\text{IR}} = 0.10$  nm depending on wavelength and alignment of the DFDL. From this and from previous measurements on the He resonance line [24] we estimate a bandwidth of  $\Delta\lambda_{\text{XUV}} \approx 0.01$  nm for the XUV source. For the probe pulse in the 1XUV + 1UV ionization scheme the 355 nm output of the same mode-locked Nd:YAG laser is used, that pumps the DFDL, so that no time jitter exists between the pump and probe beams.

The XUV and UV beams are crossed in the interaction region and intersected with a jet of gaseous  $\text{N}_2$ , obtained from a pulsed valve at a distance of 7 cm. The temporal delay between the XUV and UV pulses is controlled by spatially delaying the UV pulse on an optical rail allowing for 5.7 ns maximum delay. Lifetimes are derived from measurements, whereby the intensity of the laser-induced ion signal is integrated over 300 pulses (30 s measurement time) at each temporal delay position. The ions were collected from the interaction region by an electric field and mass separated in a field-free time-of-flight drift tube before detection. This allows for a simultaneous on-line measurement of  $^{14}\text{N}_2$  and  $^{14}\text{N}^{15}\text{N}$  isotopomers from a natural gas sample of molecular nitrogen.

Before the actual lifetime measurements were performed an excitation spectrum was recorded for each band under investigation. In Fig. 1 such a spectrum is presented for the  $c'_4(0,0)$  band. The wavelength excitation spectra were taken at zero time delay between the XUV and UV pulses. The figure demonstrates several aspects of the present method. The resolution of the laser system, indicated in the inset of Fig. 1, is much lower than in several other studies [13,15,16] and single rotational levels are not resolved; however, the resolution appears to be the same as in the study from which Shemansky et al. [6] derived rotational state dependent predissociation yields. The observed band was compared to a calculated spectrum for which rotational line strengths were used at a fitted rotational temperature of 190 K. We corrected calculated Hönl–London factors by the recently measured  $J$ -dependent oscillator strengths [26].

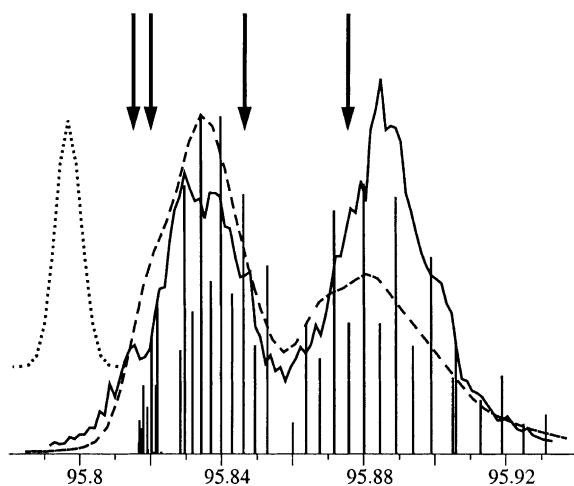


Fig. 1. Excitation spectrum (full line) and model calculation (dashed line) of the  $c'_4(0,0)$  band of  $N_2$  recorded with 1XUV + 1UV photoionization. The bandwidth profile of the XUV laser is given with the dotted curve on the same horizontal scale. The wavelengths at which lifetime measurements were performed are indicated.

The vertical spikes represent the resulting line strengths on a relative scale. By convolving with the estimated source bandwidth of  $\Delta\lambda_{\text{XUV}} = 0.01$  nm, and fitting to a relative intensity scale, a model spectrum is calculated as shown by the dashed line in Fig. 1. Reasonable agreement with the observed feature is found. It is noted that the gap in the R-branch between R(9) and R(10) (cf. [16]) is completely washed out by the limited resolution of the XUV laser. With respect to the relative underestimation of the P-branch signal it should be realized that the intensities recorded by 1XUV + 1UV photoionization are subject to the effect that the XUV-photon flux upon eighth harmonic generation in krypton may be strongly  $\lambda$  dependent. The observed spectrum nevertheless allows to give an assignment of states, or rather a distribution of states, probed while setting the XUV laser at the wavelengths marked by an arrow in Fig. 1.

A similar spectral recording was performed in the wavelength range  $\lambda_{\text{XUV}} = 93.8$ – $94.2$  nm, for the  $c'_4(1,0)$  band. Here the feature for the main isotope  $^{14}N_2$  at 94.02 nm and the one for  $^{14}N^{15}N$  at 93.90 nm were well resolved. The latter feature was overlapped by the wing of the weak  $c_3(1,0)$  band

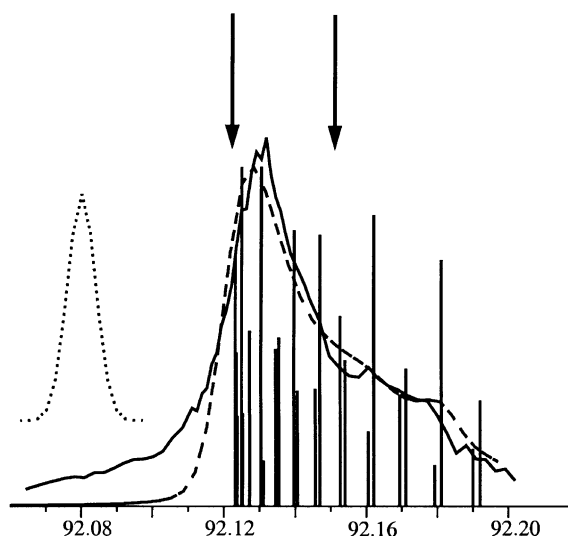


Fig. 2. Excitation spectrum (full line) and model calculation (dashed line) of the  $c'_4(2,0)$  band of  $N_2$ .

of  $^{14}N_2$  at  $\lambda = 93.87$  nm for which an indicative lifetime of  $\tau \approx 100$  ps was determined, and which will not be considered in this study. A spectral recording for the  $c'_4(2,0)$  band is reproduced in Fig. 2. For the subsequent analysis it is important to realize that at the bandhead, at the blue side ( $\lambda = 92.125$  nm), the R(0)–R(5) line overlap and in the red-shifted part of the spectrum R( $J + 6$ ) lines overlap with P( $J$ ) lines. At the wavelength position of 92.15 nm the P(4) and P(5) lines are overlapped by R(10) and R(11).

### 3. Results and interpretation

Lifetime measurements were performed for four settings in the  $c'_4(0,0)$  band: (I) at P(4)–P(8) lines; (II) at R(0)–R(5) lines; (III) and (IV) beyond the gap in the R-branch for  $J \geq 10$  with the last measurement at the very end of the R-bandhead. As an example a time delay scan is plotted in Fig. 3 with the laser set at  $\lambda_{\text{XUV}} = 95.845$  nm corresponding to position (II).

Lifetimes were derived from fitting procedures, which are described here in some detail. We calculate the signal in the two photon pump–probe experiment by first calculating the population  $n(t)$

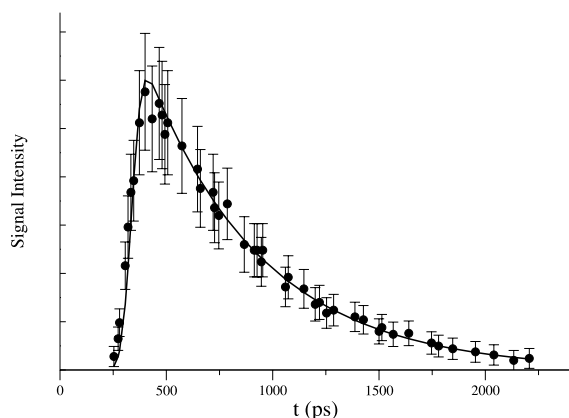


Fig. 3. Lifetime measurement with pump and variably delayed probe lasers recorded at  $\lambda_{\text{XUV}} = 95.845$  nm, covering rotational lines R(2)–R(4) in the  $c'_4(0,0)$  band of  $\text{N}_2$ . Note the linear vertical scale.

of the state, excited by the pump laser and decaying with time constant  $\tau$ :

$$n(t) = k \int_{-\infty}^t e^{-(t-\xi)/\tau} e^{-a_1^2(\xi-t_0)^2} d\xi \quad (1)$$

where  $k$  is a normalization constant. The final measured signal is proportional to the total number of ions created by the second laser pulse:

$$I(t_d) = k' \int_{-\infty}^{+\infty} \left[ \int_{-\infty}^t e^{-(t-\xi)/\tau} e^{-a_1^2(\xi-t_0)^2} d\xi \right] e^{-a_2^2(t-t_d)^2} dt \quad (2)$$

with factors  $a_i = 2\sqrt{\ln 2}/\tau_i$ ,  $\tau_i$  being the durations ( $i = 1, 2$ ) of the laser pulses (FWHM) and  $t_d$  the delay time of the ionizing pulse. In the fitting procedure all measurement points of one time delay scan are fitted simultaneously using a robust non-linear large-scale trust-region optimization method [27]. The fitting parameters are the lifetime  $\tau$ , the center-time position of the pump-pulse  $t_0$  and the scaling constant  $k'$ . The error on each measurement point consists of an error due to background and read-out noise, the fluctuations in the number of excited molecules per pulse, the error in the measurement of time delay and the statistical noise of the measurement. The resulting values for the errors are plotted as well in Fig. 3. For each scan a Monte-Carlo simulation is per-

Table 1  
Lifetimes of the  $c'_4 \Sigma_u^+$ ,  $v$  states of  $\text{N}_2$

$v$	$\tau$ (ps)	lines probed	$\lambda$ (nm)
0	$740 \pm 50$	R(0–5)	95.845
0	$650 \pm 50$	P(4–8)	95.88
0	$545 \pm 40$	R(11–13)	95.818
0	$495 \pm 50$	R(13–16)	95.820
1	$330 \pm 35$	P, R( $J < 7$ )	94.02
1	$240 \pm 35$	P, R( $J < 7$ )	93.90 <sup>a</sup>
2	$675 \pm 50$	R(0–5)	92.12
2	$680 \pm 70$	P(4–5)	92.15 <sup>b</sup>
2	$\leq 120$	R(10–11)	92.15 <sup>c</sup>

<sup>a</sup>  $^{14}\text{N}^{15}\text{N}$ .

<sup>b</sup> Bi-exponential decay, slow component.

<sup>c</sup> Bi-exponential decay, fast component.

formed by varying one third of the measured points, randomly chosen, within their  $2\sigma$ -error range assuming normally distributed errors. This is done for 100 modifications of the same scan. The distribution of the fit results for each of these scans gives an error in the range 15–50 ps, which is augmented by 20 ps to account for possible systematic effects in the lifetime measurements. The resulting uncertainties are listed in Table 1.

Specifically for the  $c'_4(0,0)$  band the issue of radiation trapping in the interaction zone was addressed. This phenomenon could play a role in the determination of the lifetime of the  $c'_4(0)$  state because (i) the oscillator strength of this band is the strongest of all in  $\text{N}_2$ , (ii) this state is the least subject to predissociation, and (iii) 90% of the emitted radiation repopulates the  $X^1\Sigma_g^+$ ,  $v = 0$  ground state. By recording lifetime decays as a function of pressure no effects were observed that could be ascribed to radiation trapping. This implies that for all other states investigated the radiation trapping can be excluded as well. However, at high pressure settings on the  $\text{N}_2$  gas pulses an increased spike of coherent two-photon ionization was observed at zero time delays. Off-resonant non-absorbing XUV can give rise to  $1\text{XUV} + 1\text{UV}$  photoionization; at higher pressure settings the resonant XUV is absorbed already outside the interaction region along the XUV beam path, thus enhancing on a relative scale the coherent off-resonant signal. This phenomenon has recently been investigated in detail on a resonance in the helium atom [34]. Although this coherent spike at

zero time delay can be deconvoluted from the observed decay functions, our measurements were preferably performed at lower pressure settings.

The results for the lifetime measurements on the lowest vibrational levels  $v = 0-2$  of the  $c'_4(1)\Sigma_u^+$  Rydberg state are listed in Table 1. Indicated are the wavelength settings of the XUV laser and the rotational lines covered by the bandwidth of the XUV source. Uncertainties are derived from the method discussed above. For the  $c'_4(0)$  state a significant variation in lifetime is found over the rotational states. For the  $c'_4(1)$  state lifetime measurements were only performed at the peak of the resonance feature; in this band the rotational structure is very congested. A lifetime for the  $^{14}\text{N}^{15}\text{N}$  isotopomer, being present only at an abundance of 0.8% in the natural nitrogen sample, could also be measured, thus demonstrating the good signal-to-noise ratio in the experiments. A clearly differing value for the lifetime of  $c'_4(1)$  is obtained.

For the  $c'_4(2)$  state lifetime measurements were performed for two different settings of the XUV laser. A first wavelength setting is chosen at the bandhead of the red-degraded band with the source bandwidth covering R(0)–R(5) lines. Then single exponential decay is observed yielding  $\tau = 675 \pm 50$  ps. At the second setting of  $\lambda_{\text{XUV}} = 92.15$  nm four rotational lines are covered by the bandwidth profile: R(10) and R(11), and P(4) and P(5) lines. The observed signal vs. pump–probe time delays at this wavelength is plotted in Fig. 4. The figure shows a clear signature of bi-exponential decay, which is indicative of contributions by excited states decaying at different rates. Analysis of the decay function yields two lifetime values, for which the slow component is assigned to the low  $J$  values, and the fast component to the higher  $J$  values ( $J = 11, 12$ ).

## 4. Discussion

### 4.1. Rydberg-valence interaction

The observed lifetimes and the  $J$ -dependences will be treated in a model based on Rydberg-

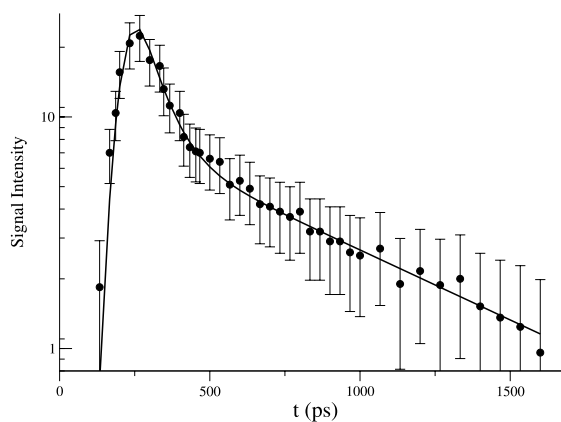


Fig. 4. Lifetime measurement for  $c'_4(2)$  at  $\lambda_{\text{XUV}} = 92.15$  nm. Note the bi-exponential decay on a logarithmic vertical scale.

valence state mixing. It has been applied by several authors [21–23,28,29] to explain lifetimes and predissociation yields in  $c'_4(3)$  and  $c'_4(4)$ . Basis of the model is the assumption that the  $3p\sigma$  and  $3p\pi$  Rydberg states (both  $c_3(1)\Pi_u$  and  $c'_4(1)\Sigma_u^+$ ) only decay radiatively, and that their predissociation behavior is induced by homogeneous and heterogeneous couplings to predissociated valence states.

Stahel et al. [14], in their seminal paper, gave a quantitative explanation of the perturbations in the dipole-allowed spectrum of  $\text{N}_2$  by relating them to Rydberg-valence state mixing. Vibronic matrix diagonalization and close-coupling methods were applied separately to three  $^1\Sigma_u^+$  ( $b'$ ,  $c'_4$ ,  $c'_5$ ) and three  $^1\Pi_u$  ( $b$ ,  $c_3$ ,  $o_3$ ) states in a diabatic representation. The vibronic matrix diagonalization method was used in a first step to optimize potentials and interaction strengths but its results were affected by the limited number of vibrational levels that were considered. Then the close-coupling method was applied as a second step taking into account the effect of a complete set of vibrational states including the vibrational continuum. The wave function of the  $c_3(0)$  state was shown by the authors to have only 34% pure  $c_3(0)$  Rydberg character, while 30% and 24% fractions of  $b(4)$  and  $b(5)$  were mixed in,  $b(v)$  denoting the  $v$  vibrational state of the  $b^1\Pi_u$  valence state.

Edwards et al. [18] have extended the model of Stahel et al. [14] by including the heterogeneous interaction between the  $c'_4(1)\Sigma_u^+$  and  $c_3(1)\Pi_u^+$  Rydberg

states which form the  $3p$  complex. Such an extension to rotational coupling between Rydberg states of  $^1\Sigma_u^+$  and  $^1\Pi_u^+$  symmetry was done initially by Helm et al. [22] in their analysis of the observed lifetimes of  $c'_4(4)$  and  $c_3(4)$  states, using the vibronic matrix diagonalization method. In Ref. [18] coupled equations were solved simultaneously for six states of both  $^1\Pi_u^+$  and  $^1\Sigma_u^+$  symmetries, adding the centrifugal terms to the potentials. In this case, the  $J$ -dependent effects and  $A$ -doubling could be accounted for. Based on the latter model, we solved again the coupled equations for the six diabatic states in the present study. As Edwards et al. [18] we used the RKR potentials generated from molecular constants given by Stahel et al. [14], and the electrostatic interactions given by the same authors. We included the heterogeneous interaction term  $(\hbar^2/\mu R^2)\sqrt{J(J+1)}$  between  $c'_4$  and  $c_3$  states as well. However, instead of employing the renormalized Numerov method as in the preceding works [14,18], we applied in the present study the Fourier grid Hamiltonian method, an efficient and accurate method for bound state problems. References and a detailed description of a similar calculation in the case of two coupled states in  $\text{Na}_2$  can be found in Dulieu and Julienne [30]. The advantage of this method is to provide all eigen values and the coupled channels wavefunctions in one single diagonalization of the hamiltonian matrix expressed in a discrete variable representation. For a given energy and a given  $J$ , the coupled channels wavefunction is given by a six-component vector, each component corresponding to a given electronic diabatic state:

$$\chi_k^d(R) = \{\chi_{ek}^d(R), \chi_{e'k}^d(R), \dots\} \quad (3)$$

The percentage of electronic character  $e$  is obtained directly from:

$$P_e^k = \int_0^\infty |\chi_{ek}^d(R)|^2 dR \quad (4)$$

The electronic component  $\chi_{ek}^d(R)$  takes into account not only the bound vibrational states but also the vibrational continuum. The percentage corresponding to a particular vibrational state of the electronic state  $e$  can be obtained by expanding  $\chi_{ek}^d(R)$  over a set of vibrational functions  $\chi_{ev}^d(R)$ ,

which are solutions of the uncoupled equation for state  $e$ :

$$P_{ev}^k = |c_{ev}^k|^2 = \int_0^\infty \chi_{ev}^d(R) \chi_{ek}^d(R) dR \quad (5)$$

For convenience of discussion, generally any given bound state can be named after its main component ( $e,v$ ) but exceptions may occur. Indeed in the case of what we named  $c'_4(2)$ , the level  $J=0$  has 50% of  $b'$  character and 50% of  $c'_4$  character, and the level with higher  $J$  has a larger  $b'$  percentage than its  $c'$  percentage. However in the energy vicinity there is no other level with a significant component of  $c'_4$  character. The results of the present calculations, in percentages  $P_e^k$  of the main electronic character versus  $J$ , are given in Figs. 5–7, for the levels named  $c'_4$ ,  $v=0, 1$  and 2 respectively. Significant contributions from other electronic states are also shown on these figures.

From the present calculations, the  $c_3$ ,  $v=0$ ,  $J=0$  level has mixing fractions of 35%  $c_3$ , 29%  $b(5)$ , 26%  $b(4)$ , 5%  $b(6)$ , 0.8%  $b(3)$  and further minor contributions. If the assumption is upheld that the pure  $c_3$  Rydberg character is unpre-dissociated, a lifetime of 740 ps and a decay rate of  $1.35 \times 10^9 \text{ s}^{-1}$  pertains for the true  $c_3$  Rydberg admixture. If decay rates for levels  $b(2)$ – $b(6)$ , taken from previous lifetime measurements [8,31], are included a total decay rate is found of  $k_{\text{tot}} = 2.15 \times 10^{10}$ , which corresponds to a lifetime of 47 ps for the perturbed  $c_3$  state. In view of the

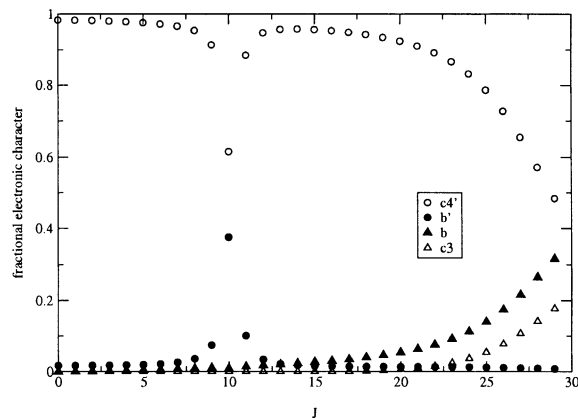


Fig. 5. Calculated mixing fractions for the  $c'_4^1\Sigma_u^+$ ,  $v=0$  state of  $\text{N}_2$  as a function of  $J$ .

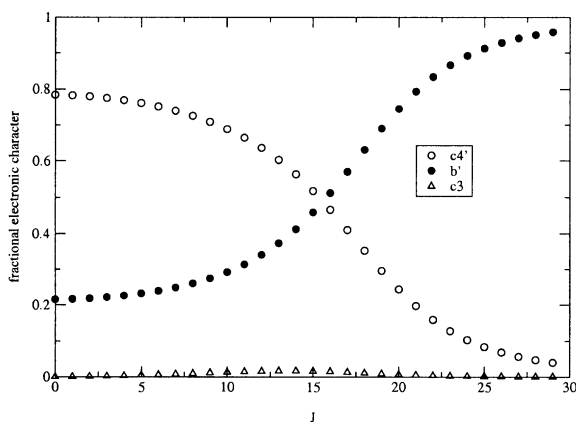


Fig. 6. Mixing fractions in  $c'_4(1)\Sigma_u^+$ ,  $v = 1$  versus  $J$ .

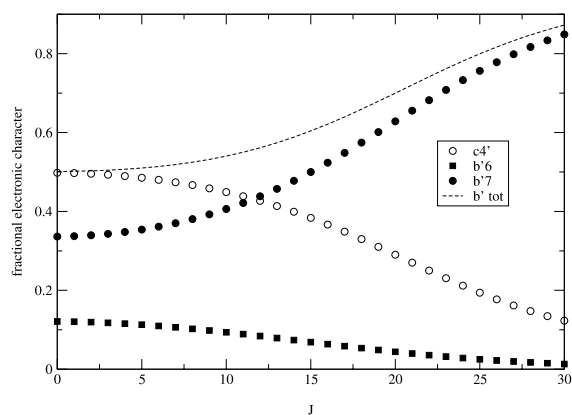


Fig. 7. Mixing fractions in  $c'_4(1)\Sigma_u^+$ ,  $v = 2$  versus  $J$ .

approximations made this value agrees reasonably well with the experimental value of 67 ps and it gives confidence for the application of the Rydberg-valence mixing model to interpret the lifetimes of other excited states. One such simplifying approximation is that the measured lifetime values also hold for the deperturbed  $b(v)$  states.

#### 4.2. $c'_4(0)\Sigma_u^+$ , $v = 0$ state

We have obtained a lifetime of  $c'_4(0)$  that tends to gradually decrease from 740 ps (for the low  $J$ -levels) toward 495 ps for  $J = 14$ – $17$  levels. The value for the low  $J$ -levels deviates somewhat from

previous measurements. While Hesser and Dressler [19] and Oertel et al. [20] found a slightly larger value, line broadening [13] yielded a smaller value. Apparently the actual XUV source linewidth in the experiment of Ref. [13] was somewhat underestimated; in view of the natural lifetime broadening effect being small with respect to the source bandwidth, this has an important effect on the deduced lifetime for the  $c'_4(0)$  and  $b(1)$  states; the findings on  $c_3(0)$  and on the relative lifetimes for  $c'_4(0)$  and  $b(1)$  are unaffected by the underestimate of the source bandwidth in Ref. [13]. It is also noted that in a derivation of the predissociation yield from the lifetime, a necessary comparison is made with an experimental value of the oscillator strength (or the radiative lifetime); these values bear error margins of at least 15% [26] that progress into the values for the derived dissociation yields. The value, presently obtained for the low  $J$ -levels in  $c'_4(0)$ , is in accordance with the combined results by Ajello et al. [2], who measured a fluorescence rate of  $1.35 \times 10^9 \text{ s}^{-1}$ , corresponding to  $\tau_{\text{rad}} = 740 \text{ ps}$ , and the finding of Shemansky et al. [6] that the low  $J$ -levels of  $c'_4(0)$  are unpredissociated. If the levels are indeed unpredissociated the lifetime of the state equals  $\tau_{\text{rad}}$  and this yields a consistent picture. The decrease in lifetime for the higher  $J$ -levels is in qualitative agreement with the observation of predissociation [6].

In Fig. 5 the calculated fractional character of the  $c'_4(0)$  state is plotted. The strong effect of mixing with the  $b^1\Sigma_u^+$  valence state is not expected to significantly affect the lifetime of  $c'_4(0)$ . The strong local perturbation at  $J = 10$  is entirely due to  $b'(1)$  and in a previous study the lifetime of  $b'(1)$  [13] was found to be even slightly larger than that of  $c'_4(0)$ , so it has no effect. The same is true for the admixture of  $c_3(0)$  Rydberg character if the assumption is upheld that the pure  $c_3(0)$  Rydberg character has the same decay rate as  $c'_4(0)$ . Thus it is postulated that the growing admixture of  $b^1\Pi_u$  valence character is responsible for the shortening of the lifetime of  $c'_4(0)$  at higher  $J$ -levels. A detailed calculation for the  $c'_4(0)$ ,  $J = 17$  level reveals in decreasing order of importance the admixtures: 95% of  $c'_4$ , 3.4% of  $b(5)$ ,  $3 \times 10^{-4}$  of  $b(4)$ ,  $7.3 \times 10^{-5}$  of  $b(6)$  and  $1.2 \times 10^{-5}$  of  $b(3)$ . It is noted that  $b(3)$ , with  $\tau = 1.6 \text{ ps}$ , is the shortest lived level [8].

Including all contributions of b(3)–b(6) and invoking the experimentally obtained lifetimes, a lifetime of 685 ps results for the  $J = 17$  level of  $c'_4(0)$ . This gives an explanation for the trend toward lower lifetime at higher rotational states, although the actually observed value of 495 ps is not fully explained.

#### 4.3. $c'_4 \Sigma_u^+$ , $v = 1$ state

The shorter lifetime of  $c'_4(1)$ , with respect to  $c'_4(0)$ , can also be explained from the perspective of Rydberg-valence mixing. In Fig. 6 the fractional electronic character for  $c'_4(1)$  is plotted, showing strong mixing with the  $b^1 \Sigma_u^+$  valence state, in this case mainly  $b'(4)$ . Note that in Fig. 6 the level identification beyond  $J = 16$  should be reversed, but this is only a matter of convention. The  $c_3$  character, mixed in at a level of 1% has no influence, while the admixture of  $b^1 \Pi_u$ , limited to a level of 0.5% only has a minor effect.

No measurements of the lifetime for  $b'(4)$  have been reported in literature. However, Ajello et al. [2] concluded from the absence of fluorescence from  $b'(4)$ , in contrast to the  $b'(3)$  state, that this state is completely predissociated. From this observation a crude limit to the lifetime of  $b'(4)$  can be set at  $\tau(b'_4) \leq 100$  ps. A detailed calculation shows that  $c'_4(1)$  has, at low  $J$ -levels, a 14% admixture of  $b'(4)$  out of an overall 22% admixture of  $b'$ . If again the pure Rydberg admixture is assumed to decay at a rate of  $1.35 \times 10^9 \text{ s}^{-1}$ , similar as for  $c'_4(0)$ , a total decay rate of the perturbed  $c'_4(1)$  state follows of  $k_{\text{tot}} = 2.45 \times 10^9 \text{ s}^{-1}$ , corresponding to  $\tau = 408$  ps, if a lifetime of 100 ps is assumed for  $b'(4)$ . From the predissociation behavior only an upper limit to the lifetime of  $b'(4)$  can be estimated. The true value may well fall in the range 60–80 ps, which would give perfect agreement with the observed lifetime for  $c'_4(1)$ ; this awaits lifetime measurements for  $b'(4)$ . Calculations, including mixing of  $b'(v)$  as well as  $b(v)$ , predict a lowering of the lifetime to 250 ps at  $J = 12$ .

The shorter lifetime of  $c'_4(1)$  in  $^{14}\text{N}^{15}\text{N}$  may relate to different admixtures of  $b'$ , due to the vibrational isotope shift in the  $b'$  state. The

spectroscopy of  $^{14}\text{N}^{15}\text{N}$  has not been investigated in sufficient detail to address this topic quantitatively.

#### 4.4. $c'_4 \Sigma_u^+$ , $v = 2$ state

In a previous study by Oertel et al. [20] a value of  $650 \pm 98$  ps was reported for the lifetime of  $c'_4(2)$ , in perfect agreement with the present finding for low  $J$  values. The  $c'_4(2)$  state is, at low  $J$ -levels, completely mixed with the  $b'$  valence state, as is shown in Fig. 7. The perturbation is mainly due to the nearby lying  $b'(7)$  level and for a fraction to  $b'(6)$ . The total  $b'$  fraction in this state is even higher than 50%, as indicated with the dashed line in Fig. 7. The  $b'(7)$  state was observed in emission [2] and a lifetime was derived in a measurement without rotational resolution [20] yielding  $\tau(b'_7) = 930 \pm 140$  ps. For the  $b'(6)$  state no lifetime is reported in literature. If it is assumed that the  $b'(6)$  is not predissociated strongly, the 12% admixture (at  $J = 0$ ) does not have a large influence. Then it is explained why the lifetime of  $c'_4(2)$ , notwithstanding the very strong valence admixture, is still of the same value as a pure Rydberg state.

The explanation for the bi-exponential decay, observed with the laser set at  $\lambda = 92.15$  nm, requires an involved argument. The slow component is consistent with the lifetime measurement at low  $J$  values, hence it is concluded that this results from probing  $J = 3, 4$  levels via the P-branch. The fast component is obviously related to the probing of  $J = 11, 12$  levels in the R-branch at  $\lambda = 92.15$  nm. An explanation for the fast component can, however, not be straightforwardly deduced from the  $J$ -dependent mixing with  $b'$  character. At  $J = 11$  the valence state fraction in  $c'_4$  is 9%  $b'(6)$ , with an increase to 42%  $b'(7)$ . In view of the observed lifetime of 930 ps for  $b'(7)$  [20] this would however have a negligible effect.

We postulate here that in the study of Oertel et al. [20] only the low  $J$ -levels were probed and that the lifetimes of the higher  $J$ -levels in  $b'(7)$  are significantly smaller. In hitherto unpublished measurements performed with the narrow-band ( $0.3 \text{ cm}^{-1}$  bandwidth) tunable XUV laser in Amsterdam evidence for such an effect was found. In

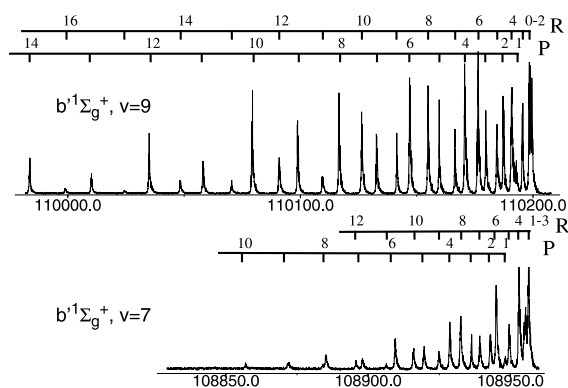


Fig. 8. High resolution 1XUV + 1UV photoionization spectra in excitation of  $b'(7)$  and  $b'(9)$  states using the Amsterdam narrowband XUV laser source.

Fig. 8 high resolution 1XUV + 1UV photoionization spectra of excitation to  $b'(7)$  and  $b'(9)$  are displayed. The spectra of the  $b'(9)$  state were published before [32]. It is essential that both spectra were recorded at precisely similar settings for the pulsed  $N_2$  beam; hence the rotational distribution at which these spectra were recorded was similar. It is obvious that the relative intensity towards higher  $J$ -levels for the  $b'(7)$  state is considerably decreased when comparing to the  $b'(9)$  state. As was shown by Eikema et al. [33] intensity loss is a signature of shorter lifetimes in 1XUV + 1UV photoionization experiments when pulsed lasers are used with durations longer than the intermediate state lifetime; the Amsterdam laser source had a pulse duration of 3–4 ns. Under such conditions the relative intensity  $I$  scales proportional with the lifetime  $\tau$  [33]. If it is assumed that the lifetime of  $b'(9)$  is independent of  $J$ , and Walter et al. [28] have provided evidence for this, the relative drop in intensity at R(10) in  $b'(7)$  by a factor of 5–6 would correspond to a lifetime of 170 ps for  $J = 11$  in  $b'(7)$ . At a mixing fraction of 42% valence character this results in a lifetime of  $\tau = 300$  ps for  $c'_4(2)$ ,  $J = 11$ . Predissociation in the high  $J$ -levels of  $b'(6)$  would then yield an even lower value. This line of reasoning does not give a full quantitative explanation for the fast component of  $\tau \leq 120$  ps, observed at 92.15 nm, but it does provide a qualitative argument for the shorter lifetime obtained.

## 5. Conclusion

Lifetime measurements for the  $c'_4(1)\Sigma_u^+$ ,  $v = 0-2$  states of  $N_2$  are presented. For  $c'_4(0)$  a  $J$ -dependence is obtained which is consistent with the observations and interpretations by Ajello et al. [2] and Shemansky et al. [6] on a rotational dependence of the predissociation yield. A model of Rydberg-valence interaction is followed explaining the observed features and the trend of the  $J$ -dependence. Here a heterogeneous state-mixing with the  $b^1\Pi_u$  state is invoked which is postulated to cause the  $J$ -dependent effects. The observed behavior in  $c'_4(1)$  and  $c'_4(2)$  is ascribed to homogeneous coupling with the  $b^1\Sigma_u^+$  state. The  $J$ -dependent effects in  $c'_4(2)$  are interpreted in terms of mixing with  $b'(7)$  for which no direct lifetime measurements are reported. However from an interpretation of hitherto unpublished data of narrow-band 1XUV + 1UV photoionization data of the  $b'(7)$  state the trend toward shorter lifetimes for high  $J$ -levels in  $c'_4(2)$  can be explained. The present work closely matches and is in line with a number of previous studies focusing on lifetimes and predissociation yields in  $c'_4(3)$  and  $c'_4(4)$  [21–23,28,29]. These models explaining the dissociation behavior in the  $c'_4$  Rydberg state all rely on mixing with  $b'(v)$  levels that are considered to be subject to interaction with continuum states at larger internuclear separation. Predissociation yields can be derived from the present data by comparing the obtained lifetimes with the radiative lifetime of  $\tau_{\text{rad}} = 740$  ps, which is at present seems the most reliable value for  $c'_4(v)$  states. Calculation of the predissociation yield  $\eta_{\text{pre}}$  via:

$$\eta_{\text{pre}} = 1 - \tau/\tau_{\text{rad}} \quad (6)$$

then gives a yield of 33% in the dissociation channel. It should be noted however that this value has, through propagation of errors, in itself a large error margin. If a 10% error in the radiative lifetime is assumed, then with the present margins of close to 10% for the observed total lifetimes, the dissociation yields are  $33 \pm 13\%$  for the higher  $J$ -levels in  $c'_4(0)$ , which would be in agreement with Ref. [6]. The finding of 330 ps for the  $c'_4(1)$  level would correspond to a predissociation yield of

55%. The  $c_4'(2)$  level, at least for the lowest  $J$ -levels, would only be marginally predissociated on the order of 10%.

### Acknowledgements

W.U., R.L. and I.V. wish to thank the Lund Laser Centre for their hospitality. This work was supported by the European Community – Access to Research Infrastructures action of the Improving Human Potential Programme, Contract no. HPRI-CT-1999-00041. Financial support from the Earth Observation program of the Space Research Organization Netherlands and Molecular Atmospheric Physics program of the Netherlands Foundation for Research of Matter is gratefully acknowledged. W. van der Zande (AMOLF Amsterdam) is acknowledged for critically reading the manuscript.

### References

- [1] R.R. Meier, *Space Sci. Rev.* 58 (1991) 1.
- [2] J.M. Ajello, G.K. James, B.O. Franklin, D.E. Shemansky, *Phys. Rev. A* 40 (1989) 3524.
- [3] D.F. Strobel, D.E. Shemansky, *J. Geophys. Res.* 87 (1982) 1361.
- [4] H.M. Stevens, *J. Geophys. Res. A* 106 (2001) 3685.
- [5] E.C. Zipf, R.W. McLaughlin, *Planet Space Sci.* 26 (1978) 449.
- [6] D.E. Shemansky, I. Kanik, J.M. Ajello, *Astrophys. J.* 452 (1995) 480.
- [7] H.M. Stevens, R.R. Meier, R.R. Conway, D.F. Strobel, *J. Geophys. Res. A* 99 (1994) 417.
- [8] W. Ubachs, L. Tashiro, R.N. Zare, *Chem. Phys.* 130 (1994) 1.
- [9] T.G. Slanger, *Planet Space Sci.* 31 (1983) 1525.
- [10] R.E. Worley, *Phys. Rev.* 64 (1943) 207.
- [11] P.K. Carroll, K. Yoshino, *J. Phys. B* 5 (1972) 1614.
- [12] J.-Y. Roncin, J.L. Subtil, F. Launay, *J. Mol. Spectrosc.* 188 (1998) 128.
- [13] W. Ubachs, *Chem. Phys. Lett.* 268 (1997) 201.
- [14] D. Stahel, M. Leoni, K. Dressler, *J. Chem. Phys.* 79 (1983) 2541.
- [15] K. Yoshino, Y. Tanaka, *J. Mol. Spectrosc.* 66 (1977) 219.
- [16] P.F. Levelt, W. Ubachs, *Chem. Phys.* 163 (1992) 263.
- [17] K. Yoshino, D.E. Freeman, *Can. J. Phys.* 62 (1984) 1478.
- [18] S.A. Edwards, W.-Ü.L. Tchang-Brillet, J.-Y. Roncin, F. Launay, F. Rostas, *Planet Space Sci.* 43 (1995) 67.
- [19] J. Hesser, K. Dressler, *J. Chem. Phys.* 45 (1966) 3149.
- [20] H. Oertel, M. Kratzat, J. Imschweiler, T. Noll, *Chem. Phys. Lett.* 82 (1981) 552.
- [21] A.W. Kam, J.R. Lawall, M.D. Lindsay, F.M. Pipkin, R.C. Short, P. Zhao, *Phys. Rev. A* 40 (1989) 1279.
- [22] H. Helm, I. Hazell, N. Bjerre, *Phys. Rev. A* 48 (1993) 2762.
- [23] J.M. Ajello, G.K. James, M. Ciocca, *J. Phys. B* 31 (1998) 2437.
- [24] J. Larsson, E. Mevel, R. Zerne, A. L’Huillier, C.-G. Wahlström, S. Svanberg, *J. Phys. B* 28 (1995) L53.
- [25] P. Cacciani, W. Ubachs, P.C. Hinnen, C. Lyngå, A. L’Huillier, C.-G. Wahlström, *Astrophys. J.* 499 (1998) L223.
- [26] G. Stark, K.P. Huber, K. Yoshino, M.-C. Chan, T. Matsui, P.L. Smith, K. Ito, *Astrophys. J.* 531 (2000) 321.
- [27] R.H. Byrd, R.B. Schnabel, G.A. Shultz, *Math. Program.* 40 (1988) 247.
- [28] C.W. Walter, P.C. Cosby, H. Helm, *Phys. Rev. A* 50 (1994) 2930.
- [29] C.W. Walter, P.C. Cosby, H. Helm, *J. Chem. Phys.* 112 (2000) 4621.
- [30] O. Dulieu, P.S. Julienne, *J. Chem. Phys.* 103 (1995) 60.
- [31] W. Ubachs, I. Velchev, A. de Lange, *J. Chem. Phys.* 112 (2000) 5711.
- [32] W. Ubachs, K.S.E. Eikema, W. Hogervorst, *Appl. Phys. B* 57 (1993) 411.
- [33] K.S.E. Eikema, W. Hogervorst, W. Ubachs, *Chem. Phys.* 181 (1994) 217.
- [34] A. Johansson et al., to be published.